

# Interparticle-Fields Amplified Radiation Reaction

Michael J. Quin,<sup>1,\*</sup> Antonino Di Piazza,<sup>1,2,3</sup> Christoph H. Keitel,<sup>1</sup> and Matteo Tamburini<sup>1,†</sup>

<sup>1</sup>Max-Planck-Institut für Kernphysik, Saupfercheckweg 1, 69117 Heidelberg, Germany

<sup>2</sup>Department of Physics and Astronomy, University of Rochester, Rochester, NY 14627, USA

<sup>3</sup>Laboratory for Laser Energetics, University of Rochester, Rochester, NY 14623, USA

(Dated: July 3, 2023)

In classical electrodynamics, energy losses due to the emission of electromagnetic radiation can be accounted for by solving the Landau-Lifshitz equation of motion. Analytically, this equation is typically solved while treating each particle independently in an external field; numerically, one often includes a self-consistent mean field, as seen with particle-in-cell (PIC) codes. In both cases, interparticle fields from point-like particles are neglected. By considering the collision of a neutral relativistic electron-positron bunch with an intense laser pulse, we demonstrate that the inclusion of interparticle fields can coherently amplify a broad range of radiated frequencies by orders of magnitude. This corresponds to an amplified energy loss by particles within the bunch, with interparticle fields that feed into the radiation reaction force.

A charged particle, for definiteness of charge  $e$  and mass  $m$ , emits electromagnetic radiation when accelerated, implying by energy and momentum conservation that the Lorentz equation should be modified. Here ‘particle’ refers to an electron  $e < 0$  or positron  $e > 0$  without distinction, and units  $\hbar = c = 1$  are used throughout. Incorporating a point particle’s self-field, which diverges on the world line, to create a self-consistent equation of motion is known as the radiation-reaction (RR) problem. In classical electrodynamics, the RR problem is tackled by solving the coupled Lorentz-Maxwell equations for a small charged sphere. In the limit of a point particle, this leads to the Lorentz-Abraham-Dirac (LAD) equation of motion [1] which, however, permits unphysical, self-accelerating solutions. This can be resolved with perturbation, by which one obtains the Landau-Lifshitz (LL) equation [2, 3]. Equations of the LAD and LL type are often solved in an external field, such as a plane wave [4], constant magnetic field [5], and Coulomb potential [6]. Yet the generalization to many particles is non-trivial.

Consider  $N$  equally spaced particles moving in a circle, which under the limit  $N \rightarrow \infty$  constitutes a steady current and emits no radiation. This starkly disagrees with the sum of energies lost by each particle if treated independently, demonstrating why the fields must be superposed before evaluating the equation of motion or Poynting vector, which vary quadratically with the fields [7–9]. This becomes essential when particles emit substantial amounts of energy coherently. Since in the LL equation the RR force is proportional to the square of the classical electron radius  $r_e = e^2/m \approx 2.8$  fm, several authors model a small bunch of  $N$  electrons with total charge  $Ne$  and mass  $Nm$  as a single particle with effective electron radius  $Nr_e$ , which would experience a coherently enhanced RR force [8, 10, 11]. This model predicts homogeneous energy loss across the bunch, which, as we will see, may lead to qualitative and quantitative inaccurate results. Schemes exist for allocating coherent energy lost to the particles *a posteriori* [12]; yet, to our knowledge,

no attempt has been made to a first-principles evaluation of the trajectories or spectrum of emitted radiation while including fields from *point-like* particles.

Here we demonstrate that the inclusion of interparticle fields when solving the LL equation for a system of point particles can amplify the radiation emitted coherently by orders of magnitude, across a broad range of frequencies. The interaction of particles with this coherently amplified radiation field correspondingly increases bunch energy losses as well as RR by individual particles. Recent experiments observing RR involve the collision of GeV-energy electrons with an ultraintense (peak intensity  $\gtrsim 10^{20}$  W/cm<sup>2</sup>), counterpropagating laser pulse [13, 14]. Instead, we leverage the interparticle fields to show that RR can become significant at MeV-energies, with barely a few thousand particles and a comparable laser.

We proceed from first principles, by employing the Liénard-Wiechert (LW) fields and solving the LL equation numerically. Consider one particle of initial four-momentum  $mu_0^\mu$  colliding with a laser of field amplitude  $F_0^{\mu\nu}$ . We employ the Minkowski metric  $\text{diag}(+, -, -, -)$  with short-hand notation  $(ab) = a^\mu b_\mu$ . Classical RR dominates the dynamics when  $R_C = \chi_0 a_0 r_e / \lambda_e \sim 1$ , where  $\lambda_e = 1/m \approx 386$  fm is the reduced Compton wavelength [15–18]. Here,  $a_0 = |e|E_0/m\omega_0$  is the normalized laser amplitude with frequency  $\omega_0 = 2\pi/\lambda_0$ , wavelength  $\lambda_0$ , and peak electric field  $E_0$ . A classical description is valid providing  $\chi_0 = \sqrt{(F_0 u_0)^2}/F_{cr} \ll 1$ , with  $F_{cr} = m^2/|e| \approx 1.3 \times 10^{18}$  V/m being the critical field of QED [15, 17, 18]. In the classical regime, the solution of Maxwell’s equations for a point particle  $i$  are given by the LW potential  $A_i^\mu(x) = [e_i u_i^\mu / (n_i u_i R_i)]_{t_i}$  evaluated at the retarded time  $t_i = t - R_i$ , which corresponds to the LW field  $F_i^{\mu\nu}(x) = \partial^\mu A_i^\nu(x) - \partial^\nu A_i^\mu(x)$  [8]. These describe the field at  $x^\mu = (t, \mathbf{x})$  from charge  $e_i$  at  $x_i^\mu = (t_i, \mathbf{x}_i)$ , separated by  $R_i = |\mathbf{x} - \mathbf{x}_i|$  in the direction  $n_i^\mu = (1, \mathbf{n}_i)$ , where  $(n_i)^2 = 0$ . By considering now  $N$  particles, the total field  $\mathcal{F}_i^{\mu\nu}(x)$  acting on the  $i$ th charge can be written

as the superposition of the external field  $F_{\text{ext}}^{\mu\nu}(x)$  and the fields from other particles excluding itself, which we refer to as interparticle fields [19]

$$\mathcal{F}_i^{\mu\nu}(x) = F_{\text{ext}}^{\mu\nu}(x) + \sum_{j=1, j \neq i}^N F_j^{\mu\nu}(x), \quad (1)$$

The trajectory of the  $i$ th charge can then be found by integrating the LL equation, which includes the self-interaction via the RR force [2]

$$\frac{du_i^\mu}{d\tau} = \frac{e_i}{m} \mathcal{F}_i^{\mu\nu} u_{i,\nu} + \frac{2r_e^2}{3m} \left[ \mathcal{F}_i^{\mu\nu} \mathcal{F}_{i,\nu\alpha} u_i^\alpha + (\mathcal{F}_i u_i)^2 u_i^\mu \right]. \quad (2)$$

The term involving the derivatives of the fields is oscillatory and smaller than QED corrections and is therefore neglected [20, 21]. To our knowledge, this system of equations has not been solved for  $N > 1$ . In this case, a closed expression for the trajectory seems unlikely. Instead, we rely on numerical solutions. With the trajectories known, one can evaluate the spectrum of emitted radiation in direction  $n^\mu = (1, \mathbf{n})$  as [22]

$$\frac{d\varepsilon}{d\omega d\Omega} = \frac{1}{4\pi^2} \left| \sum_{i=1}^N \int_{-\infty}^{+\infty} \frac{d}{dt} \left[ \frac{e_i u_i^\mu}{(n_i u_i)} \right] e^{i\omega(n x_i)} dt \right|^2. \quad (3)$$

Consider the collision of a neutral relativistic  $e^-/e^+$  bunch propagating along the positive  $z$  axis with an intense  $a_0 \gtrsim 1$ , counterpropagating laser pulse, modeled as a plane wave with potential

$$|e|\mathbf{A}_L(\varphi)/m = a_L(\varphi) [\hat{\mathbf{x}}\delta \cos \varphi + \hat{\mathbf{y}}\sqrt{1-\delta^2} \sin \varphi]. \quad (4)$$

Here  $a_L(\varphi)$  is the pulse envelope,  $\varphi = \omega_0(t+z)$  is the wave phase, and the polarization can vary between linear  $\delta = 1$  (LP) and circular  $\delta = 1/\sqrt{2}$  (CP). The maximum of the cycle-averaged square of the potential  $a_{L,0}^2/2$  is independent of polarization, for a long pulse. In the monochromatic approximation, a single particle emits a broad range of frequencies on-axis starting from  $\omega_s = D^2\omega_0/(1+a_{L,0}^2/2)$ , where  $D \approx 2\gamma_0$  and  $\gamma_0$  denote the Doppler and initial Lorentz factor, respectively [23, 24]. To achieve coherence, the laser amplitude and particles' energies should be chosen to concentrate emission at low frequencies while avoiding back-scattering, suggesting  $a_{L,0} \sim \gamma_0$ . From Eq. (3), for two copropagating particles separated by a distance  $d$  we expect a destructive fringe at frequency  $\pi/d$ . This suggests the full width at half maximum (FWHM) of the bunch should satisfy  $\text{FWHM}_b \lesssim \lambda_s/2$ , where  $\lambda_s = 2\pi/\omega_s$ , for many particles to emit coherently over a broad range of frequencies. Any coherence condition on the position should hold throughout the interaction with the laser pulse, which implies only a small initial momentum spread can be tolerated.

In our simulations, we consider a Gaussian bunch of  $\text{FWHM}_b = 16$  nm containing 4000  $e^-$  and 4000  $e^+$ , which

has an average Lorentz factor  $\gamma_0 = 5$ , rms angular spread  $\sigma_\theta = 1$  mrad and rms kinetic energy spread  $\sigma_{\text{KE}} = 0.1\%$ . Note that the average interparticle distance in the rest frame  $\approx 20a_{\text{Ps}}$  is above the Bohr radius for positronium  $a_{\text{Ps}} \approx 0.1$  nm, indicating the formation of bound states and annihilation are unlikely. Quasi-monoenergetic  $e^-$  beams with low angular spread can be produced via plasma-based particle accelerators [25, 26]. A relativistic  $e^-/e^+$  beam can then be created via the Bethe-Heitler process, as charged particles propagate through a high-Z target [27–31]. These  $e^-/e^+$  beams are typically concentrated at the low MeV energies of interest here, and contain  $\sim 1$  pC of  $e^+$  [27]. This is several orders of magnitude above our bunch, which contains  $6.4 \times 10^{-4}$  pC of  $e^+$ . A submicron, quasi-monoenergetic  $e^-/e^+$  bunch could then be created by selecting the desired energies in a magnetic chicane and compressing, without loss of charge posing a problem. This  $e^-/e^+$  bunch head-on collides with the plane-wave described by Eq. (4), with  $a_L(\varphi) = a_{L,0} \cos^2(\varphi/L)$  of domain  $\varphi \in [-\pi L/2, \pi L/2]$ . We consider two lasers which differ only by wavelength and intensity. Both lasers have amplitude  $a_{L,0} = 5$  and pulse length  $\text{FWHM}_L \approx 26.7$  fs (of intensity). The first laser has wavelength 400 nm and about  $2.2 \times 10^{20}$  W/cm<sup>2</sup> cycle-averaged intensity; frequency doubling an optical laser is a common technique and parameters exceeding ours, 30 fs pulses at intensity  $6.5 \times 10^{21}$  W/cm<sup>2</sup>, have been obtained previously at this wavelength [32]. The second laser has wavelength 100 nm and about  $3.5 \times 10^{21}$  W/cm<sup>2</sup> cycle-averaged intensity; lasers operating at this wavelength have only recently become available [33]. Quantum effects are negligible as  $\chi_0 \lesssim 3 \times 10^{-4}$  and  $\lesssim 10^{-3}$  for each wavelength 400 nm and 100 nm, respectively.

Our code numerically integrates the LL equation for each particle using a second order leapfrog scheme [20]. A small timestep  $\Delta t \approx 2.7 \times 10^{-19}$  s, one-eighth of the average interparticle distance, was needed for numerical convergence and to resolve short-range fields as well as the high frequency radiation spectrum. The code stores the historical trajectories at discrete timesteps and interpolate to find the interparticle fields at the retarded time(s). For initialization, all particles are assumed to propagate ballistically before the start of the simulation. As the interparticle distance always remains an order of magnitude above the positronium radius, the divergence of point-like particles' fields posed no difficulty in our simulations. When solving the LL equation, we consider three cases: (i) 'laser only', where particles interact only with the external field, (ii) 'laser & interparticle' fields, where particles interact with the total field [see Eq. (1)], and (iii) 'laser & intraspecies' fields, where particles interact with the external field and that generated by all other particles of the same species, but particles of different species do not interact with each other.

With the complete trajectories known, the spectrum of energy radiated can be found by a Fourier transform,

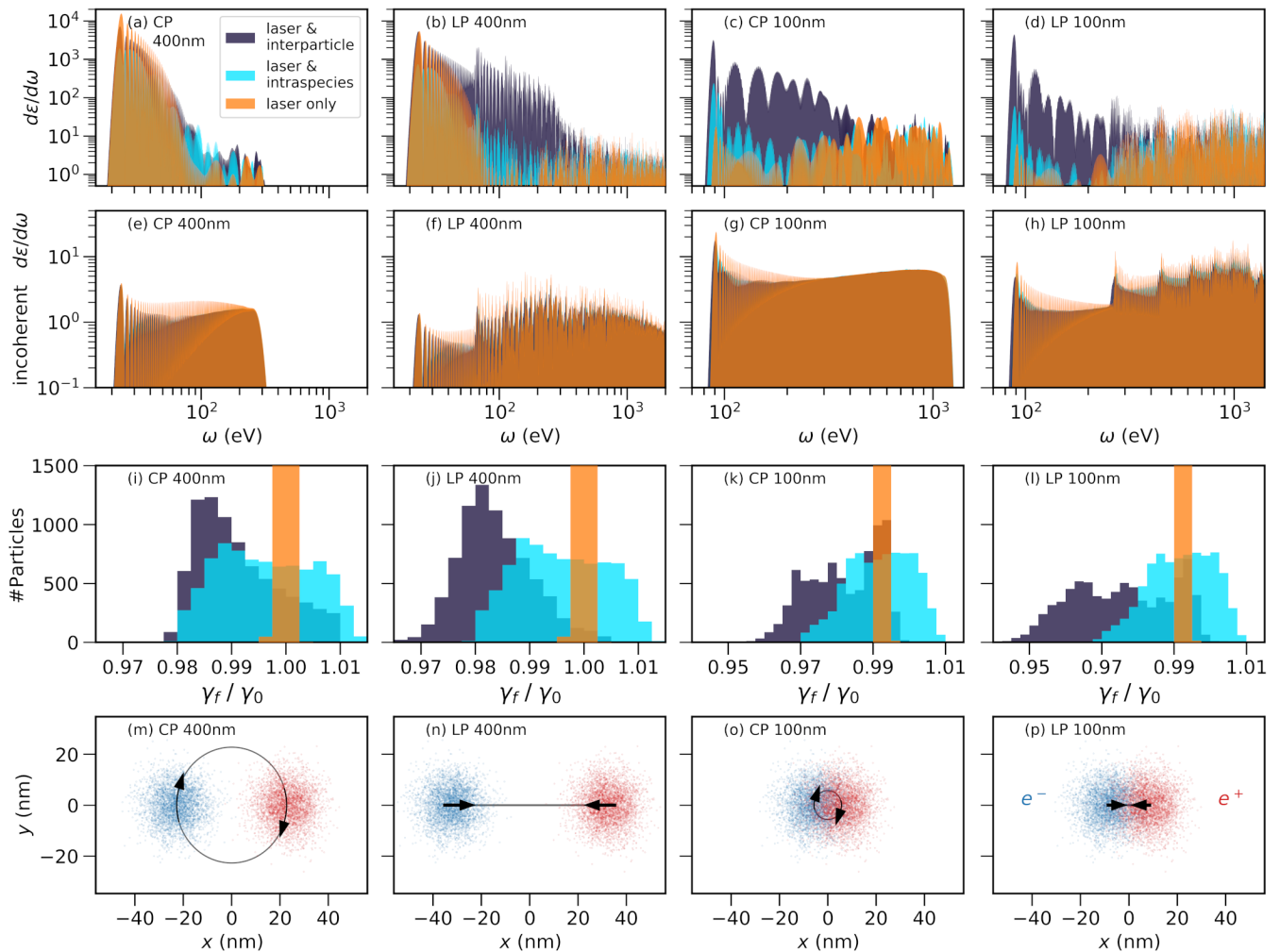


FIG. 1. (a-d) Spectrum of radiated energy integrated over the solid angle subtended by a  $1 \text{ cm}^2$  detector, at distance 1 m along the bunch velocity. (e-h) Same as (a-d) if the contribution of each particle is summed incoherently. (i-l) Final energy distribution of particles. (m-p) Schematics of the  $e^-/e^+$  dynamics in the plane perpendicular to the bunch propagation direction at the laser pulse peak. Legend in (a) applies to plots (a-l). In each column, laser varies between CP and LP, and wavelengths 400 nm and 100 nm.

which is numerically integrated over the solid angle subtended by a  $1 \text{ cm}^2$  detector, at distance 1 m along the initial velocity. Figure 1(a-d) displays the spectrum of total energy radiated for the 400 nm and 100 nm laser, for both CP and LP, and for the three considered cases ‘laser only’ (orange), ‘laser & interparticle’ (dark blue), ‘laser & intraspecies’ (light blue). Correspondingly, Fig. 1(e-h) displays the spectrum obtained if the contribution of each particle is summed incoherently, while Fig. 1(i-l) displays the final energy distribution of particles. By comparing Fig. 1(a-d) with Fig. 1(e-h), the frequencies at which the energy radiated scales coherently can be identified. In ‘laser only’, the spectra show coherence only in the 400 nm case for frequencies less than approximately 80 eV, i.e., wavelengths larger than about 15 nm [see the orange line in Fig. 1(a-h) and note that for 100 nm radiation starts at about 90 eV]. In ‘laser & intraspecies’, for

400 nm (100 nm) the spectrum is coherent for frequencies below approximately 80 eV (100 eV), with the degree of coherence below (above) the ‘laser only’ case [see the light blue line in Fig. 1(a-h)]. In ‘laser & interparticle’, the above-mentioned coherence persists. Notably, the inclusion of interparticle fields coherently amplifies frequencies from approximately 70 eV to 300 eV in all cases except for the 400 nm laser with CP, where the amplification is still present but is much milder than for LP [see the dark blue line in Fig. 1(a-h)].

Signatures of the interparticle-field amplified emission are also apparent in the final energy distribution of particles, where energy losses are substantially larger in the ‘laser & interparticle’ case [see Fig. 1(i-l)]. Hints of the physical origin of this amplification can be obtained by inspecting the particle dynamics, which is illustrated in Fig. 1(m-p) [see also the Supplemental Material (SM) at

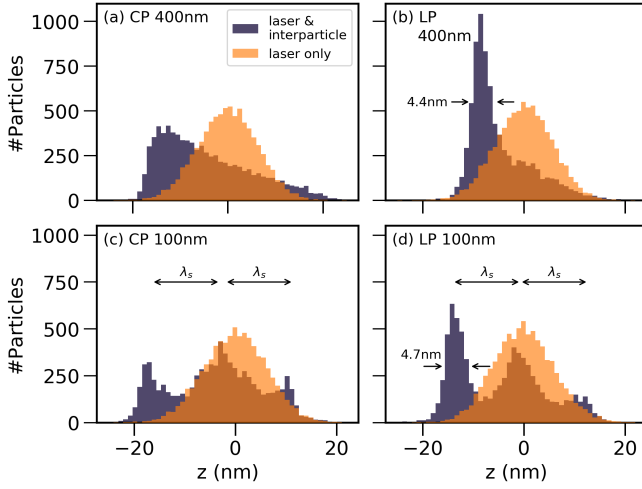


FIG. 2. Particle distribution along the bunch propagation direction  $z$  shortly after the laser pulse peak. Legend in (a) applies to all panels.

(URL) for movies of the particles' dynamics]. In fact, while  $e^-/e^+$  occupy the same volume, initially, for the 400 nm laser the two species separate transversely moving in opposite direction along the laser electric field when interacting with the pulse peak, where the field and consequently the emission is stronger. Thus, for CP the two species are separated in the plane perpendicular to the bunch propagation direction and rotate following the electric field of the laser, whereas for LP the oscillating laser electric field drives species recollision once per laser cycle [see Fig. 1(m-n) and the SM]. Conversely, for the 100 nm laser the  $e^-/e^+$  species do not separate spatially, and remain largely overlapping throughout the interaction with the laser pulse for both LP and CP [see Fig. 1(o-p) and the SM].

Figure 2 displays the distribution of particles along the bunch propagation direction  $z$  shortly after the laser pulse peak. In 'laser only' the initial shape of the particle distribution is preserved, and the observed transition from coherent to incoherent is determined by  $\text{FWHM}_b$  [see Fig. 1(a-d)]. By contrast, in 'laser & interparticle' the bunch is modulated (see Fig. 2). For the 400 nm laser with CP the bunch is just skewed toward lower energies, while with LP a peak of approximately 4.4 nm FWHM accounts for coherent emission up to 280 eV [see Fig. 2(a-b) and Fig. 1(b)]. For the 100 nm laser a triple peak structure is observed for both CP and LP, with a higher peak of about 4.7 nm FWHM with LP, while no single peak is dominant for CP [see Fig. 2(c-d)].

In Fig. 1(a-d), most of the energy radiated is concentrated at relatively large wavelengths starting around  $\lambda_s$ , which is 54 nm and 13.5 nm for the 400 nm and 100 nm laser, respectively. This corresponds approximately to the peak separation in Fig. 2(c,d). These results indicate that the orders of magnitude increase in coherent emis-

sion and amplified RR stem from the interaction of each species with the radiation produced by the other species. While the dynamics are three-dimensional as emission occurs also at large angles, a simple one-dimensional (1D) model of the energy exchange between particles and radiation field suffices to unveil the basic mechanism of bunch modulation. Following a similar reasoning as in the free-electron lasers (FELs) [34], we assume that particles' momentum is determined only by the Lorentz force and the laser field; this is a good approximation in the first part of the interaction, where emission, transverse separation of species and energy losses are small. Since the bunch is well collimated, we also assume that  $|\mathbf{p}_{\perp,0}| \ll ma_0$ ,  $|p_{z,0}|$ , where  $\mathbf{p}_{\perp,0}$  and  $p_{z,0}$  are the transverse and longitudinal initial momentum, respectively. Within the 1D model, the emitted radiation propagates approximately along the  $z$  direction and the average energy exchanged between particle and radiation as a function of the laser phase  $\varphi$  is  $dW/d\varphi = \overline{e\mathbf{p}_{\perp}(\varphi) \cdot \mathbf{E}_{\perp}(\varphi, z)}/mD\omega_0$ , where  $\mathbf{p}_{\perp}(\varphi) \approx e\mathbf{A}_L(\varphi)$ , and  $\mathbf{E}_{\perp}(\varphi, z)$  is the transverse laser and radiation electric field. Since in our approximations  $\overline{\mathbf{p}_{\perp}(\varphi) \cdot \mathbf{E}_{L,\perp}(\varphi)} = 0$ , where  $\mathbf{E}_{L,\perp}(\varphi)$  is the laser field, for  $\delta = 1$  the only relevant contribution is given by the radiation field  $\mathbf{E}_{r,\perp}(\varphi, z) = \sum_l \hat{\mathbf{x}} E_l \cos(\omega_l \varphi / \omega_0 - 2\omega_l z + \psi_l)$ , where we consider that the radiation is the superposition of several frequencies  $\omega_l$  each with its amplitude  $E_l$  and constant phase  $\psi_l$ . For a quasi-monochromatic laser pulse the average energy exchange is  $dW/d\varphi = (|e|a_{L,0}/2D\omega_0) \sum_l E_l [\cos(\eta_l) + \cos(2\varphi - \eta_l)]$ , where  $\eta_l \equiv (1 - \omega_l/\omega_0)\varphi + 2\omega_l z - \psi_l$ . A net exchange of energy is thus possible if  $\eta$  is stationary, i.e., the cycle-averaged  $d\eta/d\phi = 1 - \omega_l/\omega_0 + 2\omega_l dz/d\phi = 0$ . Since  $d\eta/d\phi = p_z(\varphi)/mD\omega_0$  and  $p_z(\varphi) \approx p_{z,0} - ma_{L,0}^2/4D$ , in the limit  $\gamma_0^2 \gg 1$  we get  $\lambda_l = 2\pi/\omega_l \approx (1 + a_{L,0}^2/4)2\lambda_0/D^2$ . Note that  $\lambda_s = (1 + a_{L,0}^2/2)\lambda_0/D^2$ . Thus,  $\lambda_l \approx \lambda_s$  for  $a_{L,0}^2 \gg 1$ .

When  $\eta_l$  is constant, there exists a sustained energy transfer between the particle and the radiation field. Depending on the particle position, the value of  $\eta_l$  changes, resulting in position-dependent rates of energy loss, which leads to the observed intrabunch modulation. This mechanism resembles that of FELs, characterized by the normalized field amplitude  $K = |e|B_0\lambda_u/2\pi m$ ,  $B_0$  and  $\lambda_u$  being the undulator field and wavelength [34], but its different nature has to be stressed. In FELs, a multi-GeV electron beam travels through an undulator with  $K \ll 1$  where monochromatic self-generated radiation copropagates with the bunch over several kms, whereas here a few MeV neutral bunch of  $e^-e^+$  travels through a 10  $\mu\text{m}$  laser pulse with  $a_0 = |e|E_0\lambda_0/2\pi m \gg 1$ , where the large-angle emission broadband radiation of one species amplifies the coherent emission of the other species. The key importance of having two species in the bunch is apparent by noting that there is basically no amplification in 'laser & intraspecies'. Furthermore, the amplified emission, in turn, results into particles experi-



encing much stronger total fields and consequently RR [see Eq. (1)]. This is prominent in the 100 nm ‘laser & interparticle’ case, where the total kinetic energy loss increases from 1.8% (1.4%) for LP (CP) with the Lorentz equation to 3% (2.3%) with the LL equation, whereas in ‘laser only’ there is no energy loss with the Lorentz equation and only 0.9% energy loss with the LL equation. Notice that plasma effects are negligible here, the particle density being about four orders of magnitude smaller than the critical density, and the skin depth being more than one order of magnitude larger than the bunch size in its average rest frame.

This article comprises part of the PhD thesis work of Michael J. Quin, which will be submitted to Heidelberg University. The authors wish to thank Brian Reville, Giuseppe Sansone, Karen Z. Hatsagortsyan, and Jörg Evers for insightful discussions.

---

\* [michael.quin@mpi-hd.mpg.de](mailto:michael.quin@mpi-hd.mpg.de)

† [matteo.tamburini@mpi-hd.mpg.de](mailto:matteo.tamburini@mpi-hd.mpg.de)

- [1] P. A. M. Dirac, Classical theory of radiating electrons, *Proc. Roy. Soc. Lond. A* **167**, 148 (1938).
- [2] L. D. Landau and E. M. Lifshitz, The classical theory of fields (Pergamon Press, Oxford, 1971) Chap. 9 §75 and §76, 3rd ed.
- [3] H. Spohn, The critical manifold of the lorentz-dirac equation, *Europhysics Letters* **50**, 287 (2000).
- [4] A. Di Piazza, Exact solution of the landau-lifshitz equation in a plane wave, *Lett. Math. Phys.* **83**, 305 (2008).
- [5] A. A. Sokolov, I. M. Ternov, and C. W. Kilmister, *Radiation from Relativistic Electrons* (American Institute of Physics, 1986).
- [6] S. G. Rajeev, Exact solution of the landau-lifshitz equations for a radiating charged particle in the coulomb potential, *Annals of Physics* **323**, 2654 (2008).
- [7] M. Abraham, Theorie der Elektrizität vol. II Elektromagnetische Theorie der Strahlung (B.G. Teubner, 1905) Chap. 2 §15, pp. 134–135.
- [8] J. D. Jackson, *Classical Electrodynamics*, 3rd ed. (John Wiley and Sons, Inc., 1998).
- [9] D. Gromes, Where the Lorentz-Abraham-Dirac equation for the radiation reaction force fails, and why the “proofs” break down, *arXiv e-prints*, 1507.05736 (2015).
- [10] P. Smorenburg, L. Kamp, G. Geloni, and O. Luiten, Coherently enhanced radiation reaction effects in laser-vacuum acceleration of electron bunches, *Laser and Particle Beams* **28**, 553–562 (2010).
- [11] A. E. Kaplan and P. L. Shkolnikov, Lasetron: A Proposed Source of Powerful Nuclear-Time-Scale Electromagnetic Bursts, *Phys. Rev. Lett.* **88**, 074801 (2002).
- [12] I. Kimel and L. R. Elias, Coherent Radiation Reaction in Free-Electron Sources, *Phys. Rev. Lett.* **75**, 4210 (1995).
- [13] J. M. Cole, K. T. Behm, E. Gerstmayr, T. G. Blackburn, J. C. Wood, C. D. Baird, M. J. Duff, C. Harvey, A. Ilderton, A. S. Joglekar, K. Krushelnick, S. Kuschel, M. Marklund, P. McKenna, C. D. Murphy, K. Poder, C. P. Ridgers, G. M. Samarin, G. Sarri, D. R. Symes, A. G. R. Thomas, J. Warwick, M. Zepf, Z. Najmudin, and S. P. D. Mangles, Experimental evidence of radiation reaction in the collision of a high-intensity laser pulse with a laser-wakefield accelerated electron beam, *Phys. Rev. X* **8**, 011020 (2018).
- [14] K. Poder, M. Tamburini, G. Sarri, A. Di Piazza, S. Kuschel, C. D. Baird, K. Behm, S. Bohlen, J. M. Cole, D. J. Corvan, M. Duff, E. Gerstmayr, C. H. Keitel, K. Krushelnick, S. P. D. Mangles, P. McKenna, C. D. Murphy, Z. Najmudin, C. P. Ridgers, G. M. Samarin, D. R. Symes, A. G. R. Thomas, J. Warwick, and M. Zepf, Experimental signatures of the quantum nature of radiation reaction in the field of an ultraintense laser, *Phys. Rev. X* **8**, 031004 (2018).
- [15] A. Di Piazza, C. Müller, K. Z. Hatsagortsyan, and C. H. Keitel, Extremely high-intensity laser interactions with fundamental quantum systems, *Rev. Mod. Phys.* **84**, 1177 (2012).
- [16] D. A. Burton and A. Noble, *Contemp. Phys.* **55**, 110 (2014).
- [17] A. Gonoskov, T. G. Blackburn, M. Marklund, and S. S. Bulanov, *Rev. Mod. Phys.* **94**, 045001 (2022).
- [18] A. Fedotov, A. Ilderton, F. Karbstein, B. King, D. Seipt, H. Taya, and G. Torgrimsson, (2023).
- [19] F. Rohrlich, *Classical Charged Particles* (World Scientific, 2007) Chap. 7.1, 3rd ed.
- [20] M. Tamburini, F. Pegoraro, A. Di Piazza, C. H. Keitel, and A. Macchi, Radiation reaction effects on radiation pressure acceleration, *New J. Phys.* **12**, 123005 (2010).
- [21] M. Tamburini, *Radiation reaction effects in superintense laser-plasma interaction*, *PhD thesis*, University of Pisa (2011).
- [22] V. N. Baier, V. M. Katkov, and V. M. Strakhovenko, *Electromagnetic Processes at High Energies in Oriented Single Crystals* (WORLD SCIENTIFIC, 1998).
- [23] E. S. Sarachik and G. T. Schappert, Classical Theory of the Scattering of Intense Laser Radiation by Free Electrons, *Phys. Rev. D* **1**, 2738 (1970).
- [24] V. Y. Kharin, D. Seipt, and S. G. Rykovanov, Temporal laser-pulse-shape effects in nonlinear thomson scattering, *Phys. Rev. A* **93**, 063801 (2016).
- [25] W. T. Wang, W. T. Li, J. S. Liu, Z. J. Zhang, R. Qi, C. H. Yu, J. Q. Liu, M. Fang, Z. Y. Qin, C. Wang, Y. Xu, F. X. Wu, Y. X. Leng, R. X. Li, and Z. Z. Xu, High-brightness high-energy electron beams from a laser wakefield accelerator via energy chirp control, *Phys. Rev. Lett.* **117**, 124801 (2016).
- [26] C. S. Hue, Y. Wan, E. Y. Levine, and V. Malka, Control of electron beam current, charge, and energy spread using density downramp injection in laser wakefield accelerators, *Matter and Radiation at Extremes* **8**, 024401 (2023).
- [27] G. Sarri, K. Poder, J. M. Cole, W. Schumaker, A. di Piazza, B. Reville, T. Dzelzainis, D. Doria, L. A. Gizzi, G. Grittani, S. Kar, C. H. Keitel, K. Krushelnick, S. Kuschel, S. P. D. Mangles, Z. Najmudin, N. Shukla, L. O. Silva, D. Symes, A. G. R. Thomas, M. Vargas, J. Vieira, and M. Zepf, Generation of neutral and high-density electron-positron pair plasmas in the laboratory, *Nature Communications* **6**, 6747 (2015).
- [28] H. Chen, F. Fiuza, A. Link, A. Hazi, M. Hill, D. Hoarty, S. James, S. Kerr, D. D. Meyerhofer, J. Myatt, J. Park, Y. Sentoku, and G. J. Williams, Scaling the yield of laser-driven electron-positron jets to laboratory astrophysical applications, *Phys. Rev. Lett.* **114**, 215001 (2015).

- [29] H. Chen and F. Fiuza, Perspectives on relativistic electron–positron pair plasma experiments of astrophysical relevance using high-power lasers, *Physics of Plasmas* **30**, 020601 (2023).
- [30] C. D. Arrowsmith, N. Shukla, N. Charitonidis, R. Boni, H. Chen, T. Davenne, A. Dyson, D. H. Froula, J. T. Gudmundsson, B. T. Huffman, Y. Kadi, B. Reville, S. Richardson, S. Sarkar, J. L. Shaw, L. O. Silva, P. Simon, R. M. G. M. Trines, R. Bingham, and G. Gregori, Generating ultradense pair beams using 400 GeV/c protons, *Phys. Rev. Res.* **3**, 023103 (2021).
- [31] A. Sampath, X. Davoine, S. Corde, L. Gremillet, M. Gilljohann, M. Sangal, C. H. Keitel, R. Ariniello, J. Cary, H. Ekerfelt, C. Emma, F. Fiuza, H. Fujii, M. Hogan, C. Joshi, A. Knetsch, O. Kononenko, V. Lee, M. Litos, K. Marsh, Z. Nie, B. O’Shea, J. R. Peterson, P. S. M. Claveria, D. Storey, Y. Wu, X. Xu, C. Zhang, and M. Tamburini, Extremely dense gamma-ray pulses in electron beam-multifoil collisions, *Phys. Rev. Lett.* **126**, 064801 (2021).
- [32] Y. Wang, S. Wang, A. Rockwood, B. M. Luther, R. Hollinger, A. Curtis, C. Calvi, C. S. Menoni, and J. J. Rocca, 0.85 PW laser operation at 3.3 Hz and high-contrast ultrahigh-intensity  $\lambda = 400$  nm second-harmonic beamline, *Opt. Lett.* **42**, 3828 (2017).
- [33] L. Drescher, O. Kornilov, T. Witting, V. Shokeen, M. J. J. Vrakking, and B. Schütte, Extreme-ultraviolet spectral compression by four-wave mixing, *Nature Photonics* **15**, 263 (2021).
- [34] P. Schmüser, M. Dohlus, and J. Rossbach, *Ultraviolet and Soft X-Ray Free-Electron Lasers*, 2nd ed. (Springer, Berlin Heidelberg, 2008).